# RSC Sustainability

## Accepted Manuscript

**RSC Sustainability**

ROYAL SOCIETY OF CHEMISTRY

ROYAL SOCIETY OF CHEMISTRY

# Towards Flexible Large-Scale Environmentally Sustainable Methanol and Ammonia Production using Industrial Symbiosis

Joshua Magson[a], Thérèse Lee Chan[b], Akeem Mohammed[b],  Keeran Ward*[a]

[a]School of Chemical and Process Engineering (SCAPE), University of Leeds, Leeds, LS2 9JT, U.K

[b]Department of Chemical Engineering, University of the West Indies, St. Augustine, Trinidad, WI.

*Corresponding author; Email: k.r.ward@leeds.ac.uk;

## Sustainability Spotlight Statement

Methanol and Ammonia are critically important building blocks for several commodities from solvents and fuels to fertilizers. Thus, defossilization at large scale is essential for cleaner production. While presently the two systems are treated independently, our study seeks to investigate industrial symbiosis as a pathway to sustainable co-production schemes utilizing cleaner, advanced technologies and greener supply chains. Here, we modeled and examined the life cycle impacts of independent production versus integrated processing, highlighting the impact of increased process efficiency and reduced resource intensity in decreasing carbon footprint while acknowledging burden-shifting. Our results align directly to the UN sustainable development goals of industry, innovation and infrastructure (SDG 9), responsible consumption and production (SDG 12) and climate action (SDG 13).

# Towards Flexible Large-Scale, Environmentally Sustainable Methanol and Ammonia Co-Production using Industrial Symbiosis.

Joshua Magson[a], Thérèse G. Lee Chan[b], Akeem Mohammed[b],  Keeran Ward*[a]

[a]School of Chemical and Process Engineering (SCAPE), University of Leeds, Leeds, LS2 9JT, U.K

[b]Department of Chemical Engineering, University of the West Indies, St. Augustine, Trinidad, WI.

*Corresponding author; Email: k.r.ward@leeds.ac.uk;

24

## Abstract

26 As industries face increasing societal and governmental pressures to adopt sustainable

27 practices, the methanol (MeOH) and ammonia ($NH_3$) sectors, significant contributors to

28 greenhouse gas (GHG) emissions, are seeking innovative solutions to transition toward

29 net-zero emissions. Here, we report on the use of industrial symbiosis (IS) as a

30 transformative strategy to facilitate the cleaner co-production of MeOH and $NH_3$ by

31 integrating green hydrogen ($H_2$) within a carbon capture and utilisation (CCUS) flowsheet.

32 We examined the environmental assessment of various co-production pathways across

33 a system boundary, which includes three (3) leading technologies -Steam Methane

34 Reforming (SMR), Autothermal Reforming (ATR) and Gas Heated Reforming (GHR),

35 considering both business-as-usual (BAU) and hybrid IS integration (*Hyd*). MeOH

36 flowsheets utilised all three technologies, while $NH_3$ production employed SMR and ATR

37 systems. This comprised of six (6) BAU MeOH and $NH_3$ co-production schemes (GHR-

38 $SMR_{BAU}$, SMR-$SMR_{BAU}$, ATR-$SMR_{BAU}$, GHR-$ATR_{BAU}$, SMR-$ATR_{BAU}$, ATR-$ATR_{BAU}$) and

39 six (6) *Hyd* (GHR-$SMR_{Hyd}$, SMR-$SMR_{Hyd}$, ATR-$SMR_{Hyd}$, GHR-$ATR_{Hyd}$, SMR-$ATR_{Hyd}$,

40 ATR-$ATR_{Hyd}$) cases, utilising cradle-to-gate life cycle assessments (LCA). Results show

41 that IS-integrated flowsheets reduced GHG emissions by 12-28% compared to BAU

42 operations, with GHG impacts improving in the order GHR-$ATR_{Hyd}$ >ATR-$ATR_{Hyd}$ >SMR-

43 $ATR_{Hyd}$ > GHR-$SMR_{BAU}$ > ATR-$SMR_{BAU}$ > SMR-$SMR_{BAU}$, in agreement with energy and

44 resource efficiency results. Notably, the GHR-$ATR_{Hyd}$ configuration outperformed all other

45 cases, reducing natural gas consumption by 11% and heating requirements by 8.3%.

46 Furthermore, sustainability results support IS as a pathway to environmental benefits-

47 with ATR-based $NH_3$ operations achieving up to 31% improved impacts linked to both

48 ecosystem quality and human health. Ultimately, our study underscores the critical role

49 of IS in advancing resilient, low-carbon practices, promoting sustainable technologies for

50 net-zero emissions and defossilisation, thereby supporting a transformative shift towards

51 sustainable industrial operations.

52

**Keywords:** Life Cycle Assessment; Industrial symbiosis, CCUS, Sustainable Industries, Energy efficiency.

## 1. Introduction

On a global scale, GHG emissions have increased by 50% over the last 30 years,[1] in which $CO_2$ emissions have increased from 22.75 billion tonnes per annum to 37.15 billion as of 2022 (63.3% increase). The Paris Agreement in 2015, amongst other legislations, set out the ambitious target to limit global temperature rises to 1.5°C and decrease global GHG emissions by 43% by 2030.[2] However, current trends in emissions and infrastructure put these commitments in jeopardy,[3] concluding that overall emissions within the chemical industry must be reduced by 60% to meet these targets.[4] As an initiative to reduce GHG emissions, chemical manufacturing companies have also agreed to cut emissions via more renewable chemical production routes, particularly weaning off the use of fossil fuel feedstocks. This is particularly apparent in the production of both MeOH and $NH_3$, which are predominantly produced from natural gas.

MeOH is considered to be one of the most important chemical raw materials and is even identified as playing an essential role in the transition from fossil fuels to renewable energy since it can be easily transported and has the potential to be an energy carrier for hydrogen storage.[5] Based on the current MeOH capacities, 90% is derived from natural gas feedstocks, predominantly via steam methane reforming (SMR), autothermal reforming (ATR) and gas-heated reforming (GHR) technology routes.[6] Globally, MeOH production has increased at a compound annual growth rate (CAGR) of 5.2%, resulting in the production rate exceeding 110 million MTPA in 2021.[1] This increasing MeOH demand has been driven by its versatility in its use as a feedstock in further chemical generation, including processing formaldehyde, acetic acid, dimethyl ether, gasoline blending and fuel cells.[7] On top of this, 40% of methanol consumption worldwide comprises energy-related uses.[8]

$NH_3$, like MeOH, is a necessary commodity chemical, and it is especially important in the fertiliser industry. It has also been identified as a liquid energy carrier, and therefore, it

82   makes it a powerful option for fuel.[9] $NH_3$ is typically produced by steam methane

83   reforming (SMR) of natural gas to produce hydrogen, which is then combined with

84   nitrogen in the Haber-Bosch process. Like MeOH, the global consumption of $NH_3$ is

85   expected to increase. In 2022, the global $NH_3$ market size was upwards of USD 202 billion

86   and is projected to surpass USD 353.3 billion by 2032 (5.8% CAGR).[10] A worldwide

87   intensification of agriculture primarily drives this expected growth to meet higher food

88   demands for a rapidly increasing population, which is expected to double by 2050.[11] Due

89   to this excessive use, $NH_3$ production releases more $CO_2$ into the atmosphere than any

90   other large-scale chemical process and accounts for 1.8% of global GHG emissions.

91   It is evident that there is a high demand for both MeOH and $NH_3$, but since both are

92   predominantly produced from natural gas, this leads to high GHG emissions, which is a

93   significant downfall. MeOH and $NH_3$ production from natural gas via SMR emits 0.62 t

94   $CO_2$e/t MeOH and 2.16 - 2.51 t $CO_2$e./t $NH_3$ respectively.[12, 13] Without changing the BAU

95   operations, which have been mostly reliant on fossil fuels, it is expected that $CO_2$

96   emissions from MeOH production will rise to 1.5 Gt $CO_2$/y by 2050.[14]

97   Co-production of MeOH and $NH_3$ allows for flexibility in plant operations and a decrease

98   in natural gas usage. High-purity $CO_2$ from the $NH_3$ plants can be used as a feedstock for

99   MeOH production via the $CO_2$ hydrogenation route, which has a lower thermal efficiency

100   compared to conventional methods.[15] The co-production scheme not only enables

101   production with overall decreased GHG emissions but creates industrial symbiotic

102   linkages between the plants since the waste $CO_2$ from the $NH_3$ plant is used as a

103   feedstock in the MeOH plant. The concept of industrial symbiosis (IS) is not new and has

104   existed for more than three decades.[16] It is a concept where resource exchanges and the

105   transactions amongst entities are mutually beneficial for all involved and has the potential

106   to create a cyclic approach to production compared to a linear transformation from raw

107   materials to production, thereby supporting a circular economy approach. Previous

108   studies have shown that IS can reduce GHG emissions and $CO_2$ emissions and create

109   an overall positive environmental impact.[17-20]

110    The waste emissions in the co-production scheme can be further reduced by considering

111    alternative energy sources. For sustainable $NH_3$ production, biochemical pathways and

112    water electrolysis using renewable sources have been investigated.[21] Similarly, multiple

113    routes for sustainable MeOH production have been investigated, which also includes

114    thermo-catalytic hydrogenation and biocatalysis.[22] However, the major challenge

115    encountered is the technology readiness level (TRL) and economics associated with the

116    alternative pathways compared to the BAU scenarios.[23] Green hydrogen ($H_2$) has shown

117    promise and is deemed a suitable alternative to fossil-based fuels.[24] There are various

118    pathways for green $H_2$ production which includes thermal, electrochemical and biological

119    primary methods.[25] Thermal and electrolysis conversion pathways for $H_2$ production have

120    been identified as the focal areas for research to achieve the targets of the production of

121    10 Mt of clean $H_2$ by 2030 and 50 Mt by 2050 based on the U.S. National Clean Hydrogen

122    Strategy and Roadmap.[26] In 2022, the global $H_2$ demand was 95 Mt and was deemed as

123    a historical high and it is estimated that this production accounted for greater than 900 Mt

124    of $CO_2$ emissions since $H_2$ was produced mainly by traditional methods. Out of this

125    demand, 50% was required for $NH_3$ and MeOH production and hence was responsible

126    for 450 Mt of $CO_2$ emissions. In the United States, SMR currently accounts for the majority

127    of the commercially produced $H_2$[27] but the country has begun putting policies in place for

128    cleaner $H_2$ production. In 2021, $9.5 billion was allocated for clean $H_2$ production and in

129    2022, additional policies and incentives were put in place to boost the country's market

130    for $H_2$ production. However, it is not expected that clean $H_2$ production methods will

131    completely replace the traditional approaches. Reasons for this include technological

132    issues with $H_2$ production, distribution and storage,[28] high cost,[29] scarcity of resources for

133    infrastructure development,[30] and the unreliability of renewable energy sources.[31]

134    Nevertheless, due to the high usage of $H_2$ in the $NH_3$ and MeOH sectors, it is anticipated

135    that a fraction of the clean $H_2$ will be integrated into these sectors and would significantly

136    reduce emissions for both production schemes. Based on the target clean $H_2$ production

137    in the United States, it is expected that there will be a hybrid system using both clean $H_2$

138    and fossil-based $H_2$. Despite the continuous effort towards a low-carbon economy, little

139    work has been done in investigating co-production schemes for commodities such as

140    MeOH and NH$_3$ and the transition to a hybrid system using both fossil-based and green

141    H$_2$. In this study, we examine the co-production of MeOH and NH$_3$ using various

142    technologies and the integration of green H$_2$ through LCAs. These results will assist in

143    charting the way forward to lower GHG emissions and more sustainable operations.

## 2. Methodology

145    This section provides a detailed overview of the modelling framework, and scenario-

146    specific descriptions applied to the integrated co-production of MeOH and NH$_3$, utilising

147    IS. Our analysis considers validated process design, for which mass and energy balances

148    were derived and used to inform life cycle assessments and energy and resource

149    efficiencies.

### 2.1 Geographical Process Boundary

151    In the United States, the chemical and petrochemical industries which are mainly

152    concentrated in the Gulf Coast, particularly in Texas and Louisiana, account for

153    approximately 40% of industrial energy consumption and emissions.[32] Louisiana is

154    renowned for its booming oil and gas and petrochemical sectors. The petrochemical

155    sector houses more than 150 petrochemical plants and 15 refineries and is therefore a

156    strategic location for process industries.[33] The majority of the plants are located in the St.

157    James Parish along the lower Mississippi River corridor between Baton Rouge and New

158    Orleans and is known as the Louisiana Chemical Corridor.[34, 35] The state possesses the

159    third highest energy consumption and the second highest energy consumption per capita

160    in the United States. In 2022, approximately 4,230 GWh of energy was generated with

161    the leading sources being natural gas and nuclear power. Renewable energy from

162    biomass, hydropower and solar energy accounted for 3.5% of the net electricity

163    generation. Approximately 70% of the available energy is consumed by the industrial

164    sector.[36] Although most of the energy is produced via natural gas, Louisiana is

165    considering alternative energy sources such as solar and offshore wind. The climate in

166    Louisiana is conducive to solar energy production since it has a high average of warm

167    and sunny days compared to other states and flat, land space is available to install solar

168    panels. Louisiana has the potential to generate up to 13,000 MW of solar power.[37]  This

169    amount of solar power is more than sufficient to provide green hydrogen for this project

170    in Louisiana. **Fig. 1** shows the approximate location of the existing chemical plants, and

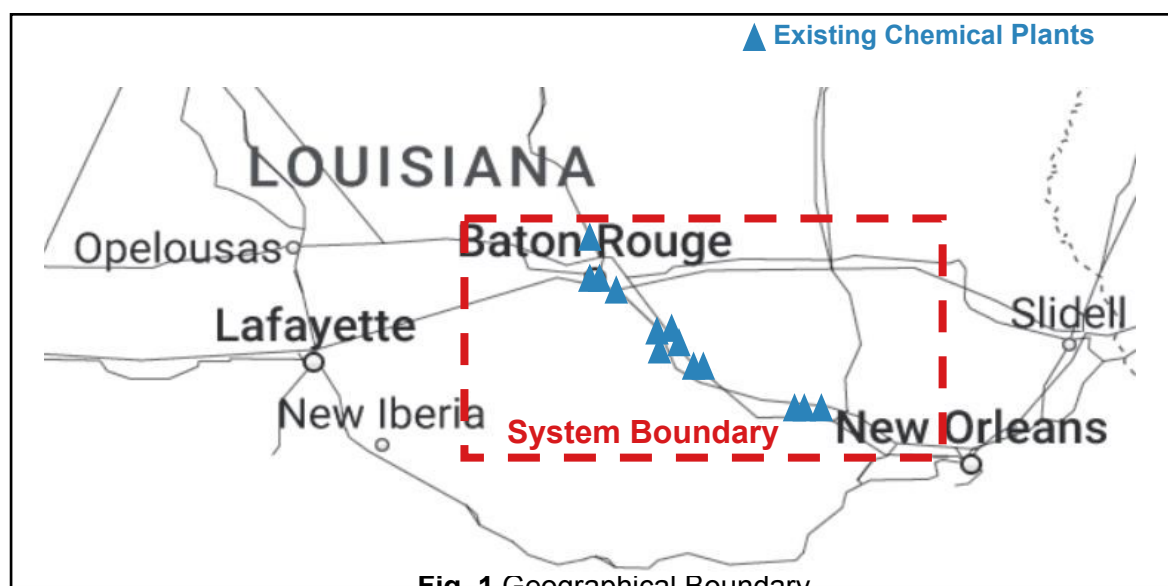171    the system boundary used in this study.



**Fig. 1** Geographical Boundary.

### 2.2. Process System Overview

189    The overall process system boundary is given in **Fig. 2.**  Technologies investigated

190    considered validated large-scale $SMR_{MeOH}$, $ATR_{MeOH}$ and $GHR_{MeOH}$ reforming operations

191    for MeOH production coupled with conventional $SMR_{NH3}$ and $ATR_{NH3}$ flowsheets for $NH_3$

192    manufacturing. Process inventories for all MeOH technologies and $SMR_{NH3}$ production

193    were taken from our previous work,[1,38] which were validated against industrial data, while

194    $ATR_{NH3}$ flowsheets were modelled using Aspen Plus (V10) process simulation software,

195    utilising the RK-Aspen property package. $ATR_{NH3}$ was considered in this study since Air

196    Liquide and KBR are partnering to develop $NH_3$ plants using  this process.[39] Thus, our

197    analysis compares six (6) business-as-usual (BAU) MeOH and $NH_3$ co-production

198    schemes (GHR-$SMR_{BAU}$, SMR-$SMR_{BAU}$, ATR-$SMR_{BAU}$, GHR-$ATR_{BAU}$, SMR-$ATR_{BAU}$,

199    ATR-$ATR_{BAU}$) and six (6) hybridised (*Hyd*) IS flowsheets (GHR-$SMR_{Hyd}$, SMR-$SMR_{Hyd}$,

7

200     ATR-SMR$_{Hyd}$,   GHR-ATR$_{Hyd}$,   SMR-ATR$_{Hyd}$,   ATR-ATR$_{Hyd}$).   For   BAU   co-production

201     schemes, conventional mega-methanol and NH$_3$ flowsheets operating at 5000 MTPD and

202     1850 MTPD, respectively, were considered as these scales were consistent with large-

203     scale MeOH and NH$_3$ production. Several industry leaders, including Johnson Matthey,

204     in conjunction with KBR, have already begun to examine the potential co-production of

205     MeOH and NH$_3$. The proposed method of integration can produce up to approximately

206     6800 MTPD of MeOH and NH$_3$ combined, and it has been shown that this co-production

207     is competitive with current industrial scales.[40]

208

209
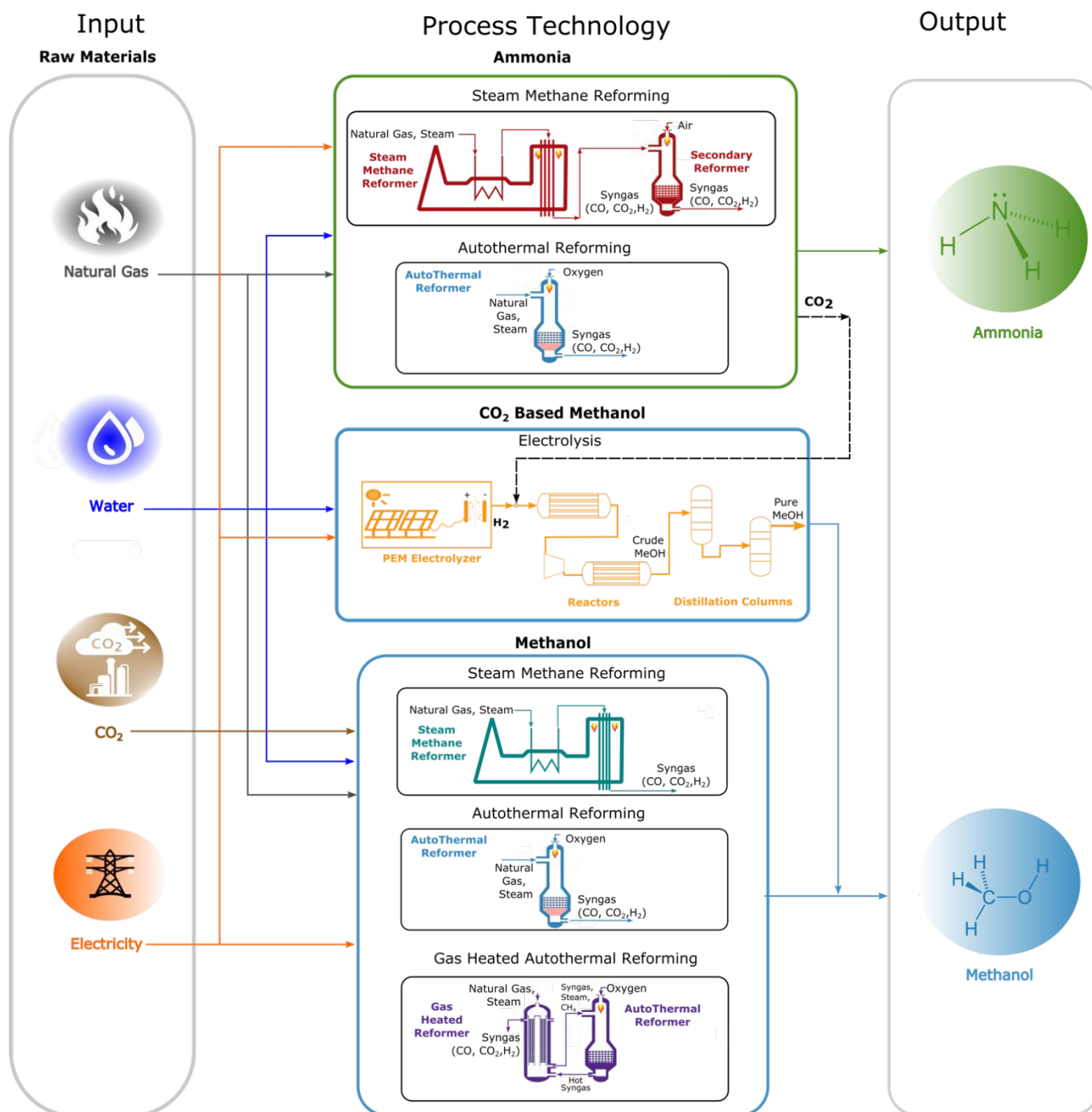
**Fig. 2** Overall process system boundary. The system includes inputs in the form natural gas, water, $CO_2$, electricity, for cleaner co-production of MeOH and $NH_3$ by integrating green $H_2$ produced via solar powered electrolysis and captured $CO_2$ from $NH_3$ synthesis.

Within the BAU co-production flowsheet, each technology was operated independently to produce both MeOH and $NH_3$ without IS.  For integrated IS flowsheets, $CO_2$ flows from both SMR and ATR $NH_3$ operations were used to produce E-methanol embedded within

216   MeOH process designs. The IS flows for each process are shown in **Table 1**. To promote

217   flexible BAU MeOH operations, fossil-based production was ramped down to support E-

218   methanol operations while maintaining large-scale capacity. Green $H_2$ feedstocks

219   required for E-methanol production were derived from solar-powered PEM electrolysis,

220   operating at an efficiency of 70.5%, a capacity factor of 0.241 and a standard enthalpy of

221   electrolysis of 39 kWh/kg$H_2$.[41] The scale of E-methanol operations was constrained to

222   270,000 tonnes/year (Total capacity =300,000 tonnes/year, on-stream factor assumed at

223   90%) in accordance with typical global E-methanol operations.[42] and the solar power

224   resource capacities of the Louisiana region. As SMR MeOH technologies utilised $CO_2$ for

225   combined steam and dry methane reforming, IS-integrated SMR-SMR$_{Hyd}$ cases required

226   external $CO_2$ feedstocks for co-production and, thus, captured $CO_2$ from natural gas

227   power plant operations were utilised. Process inventories for E-methanol production and

228   captured $CO_2$ were taken from the work by González-Garay *et al*.[41]

229

230                           **Table 1** IS Flows associated with each process

| Process/ Technology | Capacity [MTPD] | IS Flows Entering | IS Flows Exiting |
|---|---|---|---|
| SMR$_{MeOH}$ | 5000 | $CO_2$ | None |
| ATR$_{MeOH}$ | 5000 | None | None |
| GHR$_{MeOH}$ | 5000 | None | None |
| E-Methanol | 822 | $H_2$, $CO_2$ | None |
| SMR$_{NH3}$ | 1850 | None | $CO_2$ |
| ATR$_{NH3}$ | 1850 | None | $CO_2$ |

231

232 **2.2.1 ATR$_{NH3}$ Process Development**



233
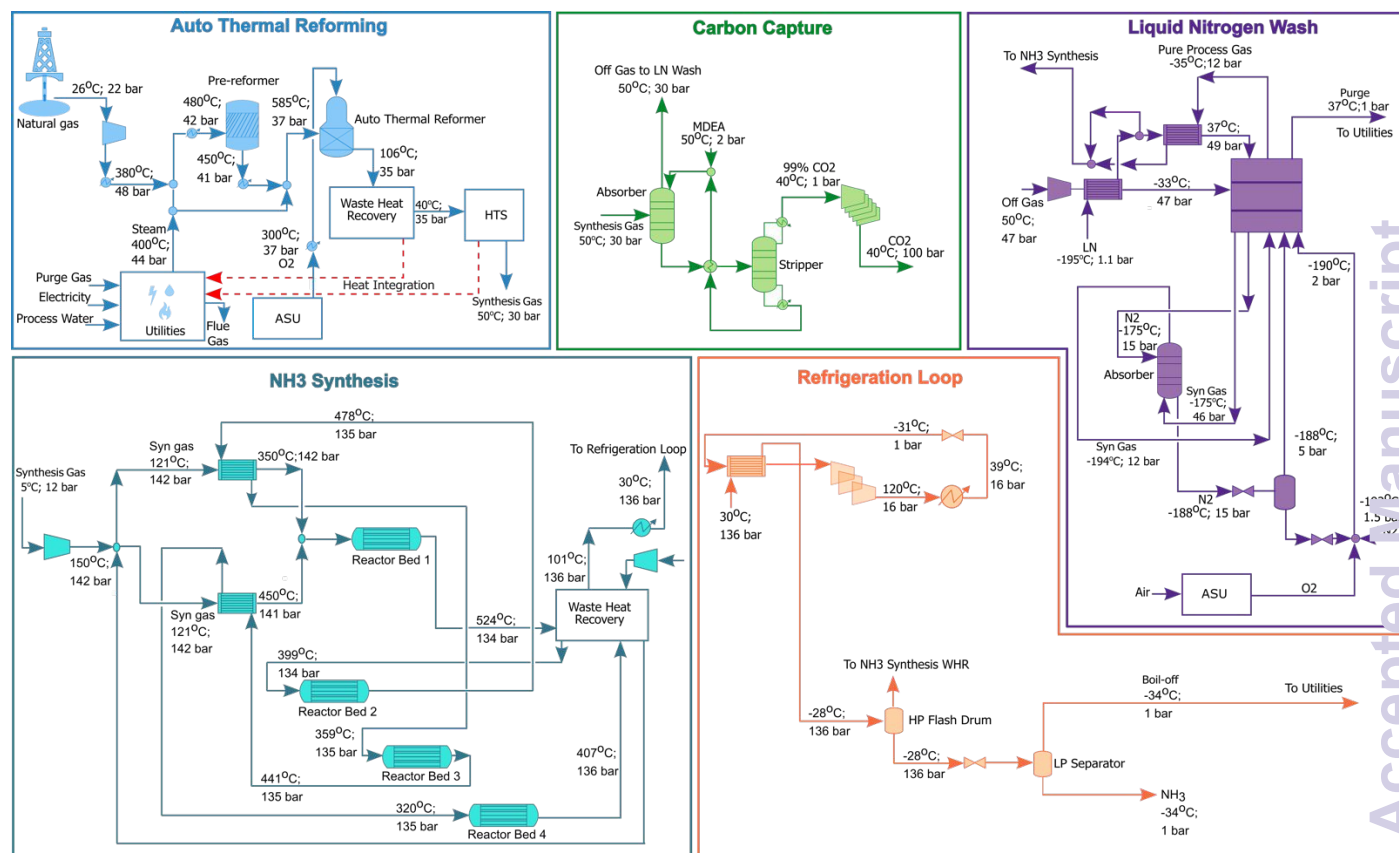
234    **Fig. 3** Overall ATR$_{NH3}$ flowsheet consisting of five (5) unit operations, including auto-thermal

235 reforming, carbon capture, liquid nitrogen wash, ammonia synthesis and product removal using

236 refrigeration. Process integration is linked throughout, illustrating the transfer of purge gases

237 and boil-off for energy recovery as well as heat recovery across synthesis and reforming

238 sections.

239

240 The overall ATR$_{NH3}$ flowsheet is given in **Fig. 3**. The front-end plant model followed

241 standard ATR-based H$_2$ production according to available literature.[43, 44] Desulphurised

242 natural gas was compressed to 49 bar and mixed with medium-pressure (MP) steam at

243 a steam-to-carbon ratio of 0.6. This mixed feed gas was preheated to pre-reforming

244 conditions (480°C), allowing for the methanation of higher hydrocarbons (eqns (1-4)),

245 creating a lean methane-rich feed gas for autothermal reforming. The lean feed gas was

246 mixed with preheated oxygen (99.5% mol, 300°C) and reacted in an adiabatic ATR unit.

247 Methane partial oxidation (eqns (6-7)) occurs simultaneously with reforming reactions

248 (eqns (4-5)), providing the thermal energy required for steam reforming. The hot reformed

11

249  gas was then cooled through waste heat recovery, mixed with auxiliary MP steam and

250  reacted across two high-temperature water-gas shift converters, where CO is converted

251  into $CO_2$ (eqn (4)). The resulting $H_2$-rich gas was further cooled and sent to $CO_2$ removal.

252

$$C_2H_6 + 2H_2O \rightarrow 2CO + 5H_2, \qquad \Delta H = 346.6 \; kJ/mol \qquad (1)$$

$$C_3H_8 + 3H_2O \rightarrow 3CO + 7H_2, \qquad \Delta H = 499.0 \; kJ/mol \qquad (2)$$

$$CO + 3H_2 \leftrightarrow CH_4 + H_2O, \qquad \Delta H = -205.9 \; kJ/mol \qquad (3)$$

$$CO + H_2O \leftrightarrow CO_2 + H_2, \qquad \Delta H = -41.1 \; kJ/mol \qquad (4)$$

$$CH_4 + H_2O \leftrightarrow CO + 3H_2, \qquad \Delta H = 205.9 \; kJ/mol \qquad (5)$$

$$CH_4 + 2O_2 \rightarrow CO_2 + 2H_2O, \qquad \Delta H = -401.4 \; kJ/mol \qquad (6)$$

$$CH_4 + O_2 \rightarrow CO + H_2 + H_2O, \qquad \Delta H = -277.9 \; kJ/mol \qquad (7)$$

260  The $CO_2$ removal unit was modelled based on our past work,[7] assuming a rate-based

261  methyl-diethanolamine (MDEA) capture system with a 90% capture efficiency and

262  normalised heating and cooling demands of 5.7 and 6.2 kJ/kg $CO_2$. The sweet synthesis

263  gas leaving the $CO_2$ removal unit was sent to an adsorber where residual $CO_2$ and

264  moisture were removed. The dried synthesis gas is chilled to -175°C through a triple

265  cascade counter-current heat exchange system and washed with liquid nitrogen, where

266  inerts are completely removed. The final purified gas was mixed with gaseous nitrogen,

267  ensuring a 3:1 ratio of $H_2$:$N_2$ required for $NH_3$ synthesis. The liquid nitrogen system was

268  modelled using the conditions described by Haonan *et al*.[45]

269

270  The back end section of the ATR $NH_3$ flowsheet considered a traditional Haber-Bosch

271  process,[46] whereby $N_2$ and $H_2$ react to produce $NH_3$ over an iron catalyst at 141 bar and

272  450°C (eqn (8)). The $NH_3$ synthesis unit consists of 4 adiabatic-packed bed reactors,

273  integrated with heat recovery and MP steam generation which effectively removes the

274  heat of reaction. The reactor model followed Temkin and Pyzhev kinetics,[47] imported into

275  Aspen Plus. The cooled effluent from the synthesis section was chilled to -33°C using an

276  $NH_3$ refrigeration cycle and flash separated at 1 bar to yield 100% pure product $NH_3$.

277
$$\frac{1}{2}N_2 + \frac{3}{2}H_2 \leftrightarrow NH_3, \qquad \Delta H = -45.6 \; kJ/mol \qquad\qquad (8)$$

278
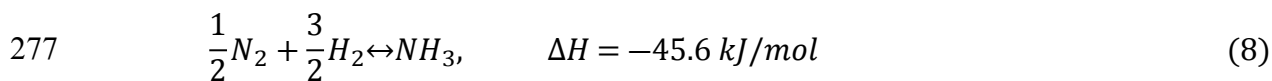
279 The utilities section of the ATR process included heat recovery through steam generation,

280 power generation, heating and cooling. Steam generated within the front and back end

281 was used as feedstock for steam reforming and heating within $CO_2$ removal and liquid

282 nitrogen wash units. Purge gas arising from the liquid nitrogen wash and low-pressure

283 $NH_3$ boil-off was combusted, providing heating duties within the front end and power

284 generation for process operations, considering a standard Rankine cycle with an

285 efficiency of 30%.

286

287 **2.3 Life Cycle Assessment (LCA)**

288 To investigate the environmental impacts associated with each scenario-specific co-

289 production scheme, a cradle-to-gate LCA methodology was applied, utilising the ISO

290 14040:2006 framework. In accordance with the ISO framework, the assessment

291 methodology is conducted across four (4) levels. _Level 1: Goal and Scope_. The goal and

292 scope of our study considers twelve (12) MeOH-$NH_3$ co-production system boundaries

293 (**Fig. 3**), considering independent BAU MeOH and $NH_3$ co-production pathways as well

294 as IS integrated schemes. As illustrated, $CO_2$ is the main IS flow, and it is combined with

295 green $H_2$ to produce E-methanol, allowing for integrated waste-to-resource value chains.

296 As the aim of our study is to examine climate-friendly $NH_3$ manufacturing, the functional

297 unit was set as 1 kg $NH_3$ produced from each co-production scheme. _Level 2: Life Cycle_

298 _Inventory Analysis (LCI)._ Scenario-specific inventories were defined from the integration

299 of both technologies as described previously in **Section 2.2**, with foreground system

300 inventories derived from literature data[1, 38, 41] and process simulations. In contrast,

301 background supply chain inventories were taken from Ecoinvent databases. Economic

302 allocation was used to distribute burdens between co-products, as neither system

303 boundary expansion nor substitution were deemed favourable allocation approaches due

304 to the complexity of the integrated flowsheets. The input-output structure is defined in **Fig.**

305 **2**, which illustrates the mass and energy flows for each technology. The inputs consisted

306 of natural gas (both as a feedstock and utility), water, electricity, captured $CO_2$ and green

13

307  $H_2$. Outputs were co-products of MeOH and $NH_3$, process-based ($CO_2$ removal in $NH_3$

308  technologies), and other $CO_2$ emissions arising from fuel combustion for heating and

309  power generation within technologies. Detailed normalised inventories are given in **Table**

310  **2** in the **Results and Discussion Section**.

311

312  *Level 3: Life Cycle Impact Assessment (LCIA).* In the LCIA stage of our study, both

313  midpoint and endpoint characterisation methods were used, following the ReCiPe 2016

314  Hierarchist-H method, using SimaPRO LCA software. The Hierarchist (H) perspective

315  method was deemed the most appropriate for our research, allowing for easier, quantitative

316  comparison of the environmental burdens associated with each of our cases.[48]  While the

317  ReCiPe (H) midpoint characterisation considers 18 impact categories, only GHG missions

318  (Global Warming Potential) were investigated for our study. However, to analyse the

319  impact of potential burden-shifting within impact categories, endpoint characterisation

320  was examined across three main areas- human health, ecosystem quality and resource

321  depletion. The full LCIA results of all cases are given in **Supplementary Data, Section**

322  **2**. *Level 4: Interpretation.* By comprehensively analysing the LCIA at both the midpoint

323  and endpoint, decision variables can be used to compare BAU co-production schemes

324  with IS-integrated flowsheets through multiple decision-making criteria (**see Results and**

325  **Discussion Section 3.4**), guiding achieving cleaner large-scale $NH_3$ manufacturing.

326

## 3. Results and Discussion

328  This section presents the results summary and analysis over five (5) main sections: LCI

329  overview and Analysis, Energy and Resource Performance, LCIA, and Multiple Decision-

330  Making Criteria. Twelve (12) MeOH and $NH_3$ co-production schemes were modelled and

331  defined by mass and energy balances, correlated by key performance indicators and

332  characterised by thermodynamic profiles and environmental burden quantification. By

333  analysing hotspots and trade-offs within each case-specific model, multiple decision-

334  making criteria were applied, revealing the most environmentally sustainable route to eco-

335  friendly $NH_3$ production at scale.

336

### 3.1 LCI Overview and Analysis

Considering the overall performance of each technology, **Table 2** gives an overview of the normalised mass and energy balance profiles for both BAU and IS-integrated (*Hyd*) co-production flowsheets. Focusing on BAU processes across all cases, $SMR_{NH3}$ technologies utilise, on average, approximately 17% more natural gas input and three times as much heat than $ATR_{NH3}$ cases. This is mainly attributed to the heating needs of SMR operations, both for primary and secondary reforming and steam production within both MeOH and $NH_3$ production. Looking closely at individual operations, $ATR_{NH3}$ utilise 40% more water than $SMR_{NH3}$ cases due to the increase in CO shift conversion arising from autothermal reforming and partial oxidation but requires 41% less cooling needs due to efficient heat recovery. Although $ATR_{NH3}$ flowsheets produce 20% more process $CO_2$ than $SMR_{NH3}$ operations, they require no additional heating needs, and thus, this increase in energy efficiency accompanies a 33% reduction in total $CO_2$ produced. Overall, $NH_3$ technologies consume less electricity than MeOH technologies, such as GHR units, where trade-offs between heating and electrification are required for pumping and compression. For IS integrated flowsheets, the inherent flexibility of MeOH operations accompanied reductions in natural gas utilisation (11%) and heating (8.3%) but an 8% increase in electricity consumption due to E-methanol operations. This decrease in the use of resources coupled with $CO_2$ utilisation saw an average 28% reduction in total $CO_2$ emissions across all IS cases compared to BAU operations. Ultimately, trade-offs between electrification and heating pose the greatest benefits in contributing to low-carbon $NH_3$ production, with the GHR-$ATR_{Hyd}$ boasting net zero heating and the lowest recorded natural gas usage, cooling duties and total $CO_2$ emissions across all co-production cases.

### 3.2 Energy and Resource Efficiencies

The process performance of all co-production cases was analysed using energy efficiency (EE) and resource intensity (RI) KPIs, given in eqns (9-10) below:

$$EE = \frac{\sum_p^n F_p . NHV_p}{\sum_i^n F_i . NHV_i + E_{Grid}} \tag{9}$$

15

366 $$RI = \frac{F_{Natgas}.NHV_{Natgas}}{\Sigma_p^n F_p}$$ (10)

367   where, $F_{i,p,Natgas}$ is the mass flow (kg/s) of raw materials, products, natural gas, $NHV_{i,p,natgas}$

368   is the heating value of raw materials, products, natural gas, $E_{Grid}$ is the electricity

369   consumption from the Louisiana power grid.

370   EE of a given process outlines the energy conversion rate from inputs to outputs, while

371   RI shows the use of fossil fuel resources in producing both MeOH and $NH_3$. Thus, an

372   increase in EE and a decrease in RI give a more energetically and resource-efficient

373   process flowsheet, favouring greater sustainable operations. The results of EE and RI

374   across all cases are presented in **Fig. 4**. In alignment with the process systems overviews

375   provided in **Section 3.1**, general trends show EE increases and RI decreases in the order

376   GHR>ATR>SMR, with $ATR_{NH3}$ technologies outperforming $SMR_{NH3}$ cases. Focusing on

377   BAU flowsheets, SMR-SMR$_{BAU}$ gives the highest RI and lowest EE at 35 MJ/kg$_{Product}$ and

378   61.5%, respectively. In contrast, GHR-ATR$_{BAU}$ was the most energetically favourable at

379   an RI of 25.89 MJ/kg$_{Product}$ and EE at 79.6%. Comparing like-for-like MeOH technologies

380   across $NH_3$ flowsheets, EE improves between 17.1 -19%, and RI decreases between

381   15.3-17.2% with the adoption of $ATR_{NH3}$ production. Similar results are observed

382   considering hybrid operations, with GHR-ATR$_{Hyd}$ operations outperforming all other cases

383   at an EE of 80.1% and RI at 25.74 MJ/kg$_{Product}$. Notably, hybrid flowsheets do not suffer

384   much energy penalties, with EE increasing within the range of 0.58-1.9% compared to

385   BAU processes. This indicates the synergy between both flowsheets to support co-

386   production. Although IS provides pathways towards efficient energy utilisation, it is

387   important to note that GHR-ATR$_{BAU}$ systems outperform all other cases except its own

388   hybrid flowsheet GHR-ATR$_{Hyd}$ - at most a 30% increase in EE and a 27% decrease in RI,

389   promoting the need for greater energy analysis and trade-off assessment in co-production

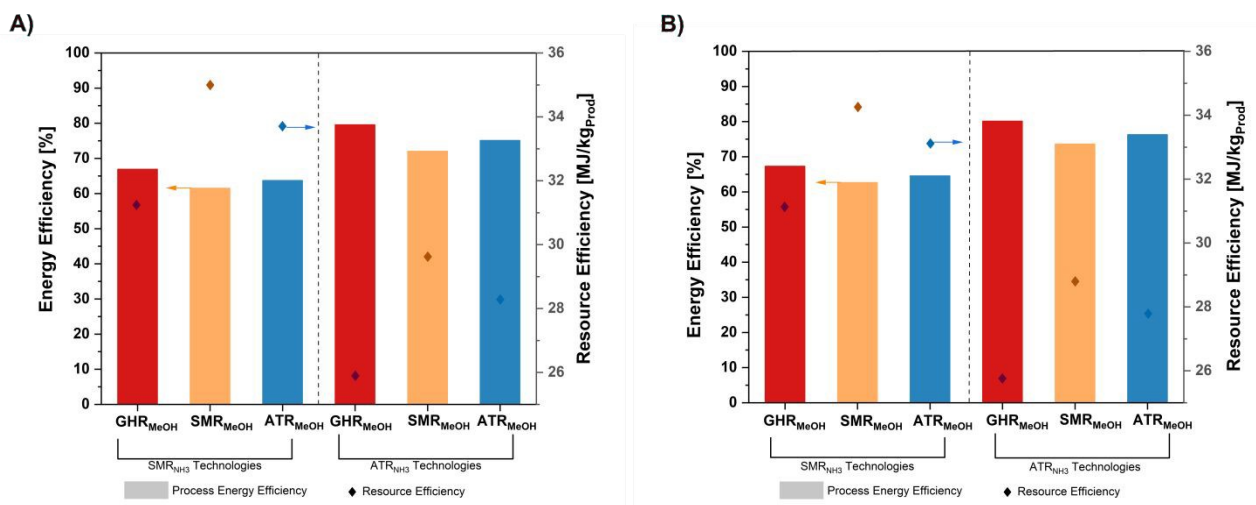390   schemes.

Fig. 4 Energy and resource efficiencies. A) BAU cases, B) IS integrated (*Hyd*) cases.

### 3.3 LCIA

#### 3.3.1 GHG Impact

The LCIA results are given for different IS-integrated MeOH-NH$_3$ co-production flowsheets and BAU processes as outlined in **Fig. 5**. For BAU co-production schemes, the main hotspots identified were linked to natural gas consumption (22-26%) and direct CO$_2$ emissions (process + other) arising from co-production operations (53-75%). Minor GHG contributions cumulating 3-27% were attributed to electricity and water consumption. For all inventories, environmental burdens arise from releasing CO$_2$, CH$_4$ and N$_2$O across raw material supply chains, consistent with raw material extraction and processing, fossil fuel consumption and fugitive emissions. Across BAU cases, SMR$_{NH3}$ technologies performed worse than ATR$_{NH3}$, with the highest GHG burdens of 1.23 kgCO$_2$e/kg$_{NH3}$ assigned to SMR-SMR$_{BAU}$ co-production. At the same time, the most significant reduction in GHG (28%) was observed for GHR-SMR$_{BAU}$, mainly due to lower direct CO$_2$ emissions associated with GHR operations.

Similar results were observed across hybrid co-production cases, with the main hotspots, natural gas consumption (22-26%) and direct CO$_2$ contributions (38-65%), being marginally lower. Furthermore, the addition of green H$_2$ and captured CO$_2$ added little to the overall GHG impact (1.1-11%), as consolidated impacts were heavily outweighed by reduced GHG burdens due to decreased natural gas utilisation and minimised process-

17

413    based $CO_2$ emissions. Although overall performance followed similar trends at the BAU

414    level, hybrid cases produced 12% less GHG emissions on average than BAU cases - with

415    GHR-ATR$_{Hyd}$ performing the best (0.76 kgCO$_2$e/kg$_{NH3}$). Notably, despite the apparent

416    benefits of IS, hybrid SMR$_{NH3}$ technologies' GHG burdens exceeded ATR$_{NH3}$ BAU cases,

417    illustrating the need to move towards ATR-based ammonia operations. Ultimately, GHG

418    impacts improve in the order GHR-ATR$_{Hyd}$ >ATR-ATR$_{Hyd}$ >SMR-ATR$_{Hyd}$ > GHR-SMR$_{BAU}$

419    > ATR-SMR$_{BAU}$ > SMR-SMR$_{BAU}$, in agreement with energy and resource efficiency

420    results.  While IS benefits are only realised through the integration of green $H_2$, the

421    flexibility of IS-integrated co-production flowsheets will likely support larger E-methanol

422    integration as renewable electricity is scaled up, allowing for greater sustainable

423    operations of MeOH and $NH_3$ manufacturing.

424

425    **3.3.2 Burden-Shifting Analysis**

426    As IS supports decreased GHG impacts and resource intensities at the co-production

427    level, it may accompany burden-shifting to other impact categories compared to BAU

428    operations due to the integration of new feedstocks.  Considering all midpoint categories

429    (**see Supplementary Data, Section 2**), burden-shifting is apparent across most impact

430    categories, including ionising radiation, ozone formation, particulate matter, ecotoxicities,

431    acidification, eutrophication, fossil resource scarcity and water consumption. At the

432    endpoint, impacts were consolidated with human health burdens linked to particulate

433    matter, ecotoxicities, ozone depletion, eutrophication, and acidification attributed to

434    ecosystem quality. In contrast, global warming, ionising radiation and particulate matter

435    are shared. Burdens affiliated with water consumption, fossil and mineral depletion and

436    land usage are linked to resource scarcity. These burdens were mainly attributed to

437    mining and mineral extraction, as well as materials production and fabrication, which

438    released harmful compounds such as copper, zinc, antimony, lead, and arsenic, as well

439    as radioactive sources, nitrogen oxides, phosphates and $SO_2$ into the environment.

440    Focusing on endpoint impacts (**Fig. 5(B-C)**), burdens associated with natural gas

441    consumption were reduced by 11%, moving away from BAU operations – with improved

442    IS contributions to human health and ecosystem quality ranging from 26-31% and 23-

443    26%, respectively. These results were particularly noticeable in resource scarcity, where

444    natural gas consumption dominated the burden contribution, ranging from 88-99%. Unlike

445    the other endpoint impact categories, burden-shifting was not observed in resource

446    scarcity– with technological performance following the same trends as described for GHG

447    impact (Best case, GHR-ATR$_{Hyd}$ = 0.133 USD$_{2013}$/kgNH$_3$; Worse case, SMR-SMR$_{BAU}$ =

448    0.182 USD$_{2013}$/kgNH$_3$). However, additional E-methanol operations worsen human health

449    and ecosystem quality burdens, with green H$_2$ and increased electricity consumption

450    leading to an increase in human health and ecosystem quality by 7% and 3%,

451    respectively. Overall, ATR flowsheets performed the best across both human health

452    (ATR-ATR$_{BAU}$ = 1.19x10$^{-6}$ DALY/kgNH$_3$) and ecosystem quality (ATR-ATR$_{BAU}$ = 2.91x10$^{-9}$

453    species-yr/kgNH$_3$) and while GHR and SMR technologies performed the worse (GHR-

454    SMR$_{Hyd}$ =1.67x10$^{-6}$ DALY/kgNH$_3$; SMR-SMR$_{Hyd}$ = 4.06x10$^{-9}$ species-yr/kgNH$_3$).
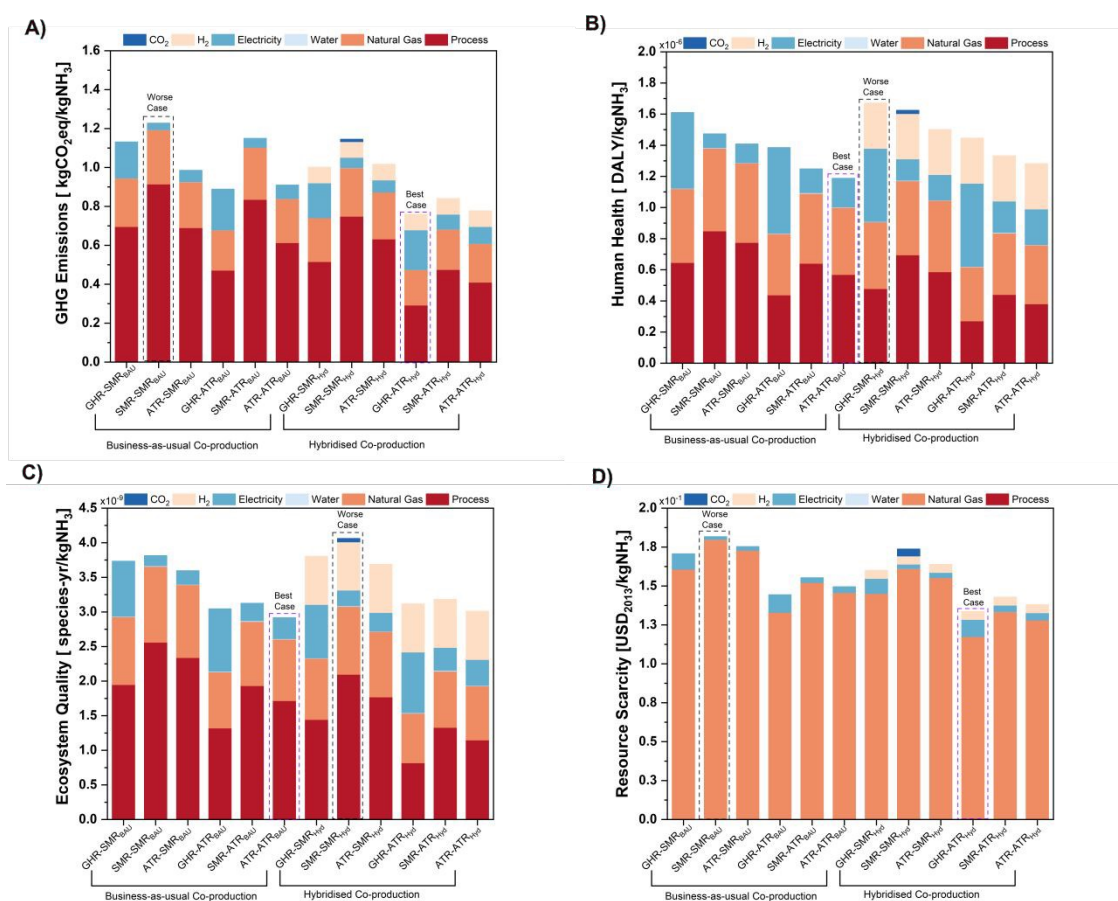


455

456    **Fig. 5** LCIA results for all co-production cases across four (4) main categories including, A)

457        GHG emissions, B) Human health, C) Ecosystem quality and D) Resource scarcity.

19

458      **3.4 Multiple Decision-Making Criteria**

459      Normalised spider plots, as shown in **Fig. 6**, were developed to assist in a multi-criteria

460      decision-making approach for evaluating the sustainability of the co-production systems.

461      The indicators, which consisted equal weights of both environmental and process, were

462      resource scarcity, ecosystem quality, human health, GHG emissions and process

463      efficiency. The reverse score was used for process efficiency since this indicator should

464      be maximised, compared to all the other indicators, which should be minimised.

465      Therefore, the largest area in the normalised spider plots will represent the most inferior

466      co-production system.

467



468
469
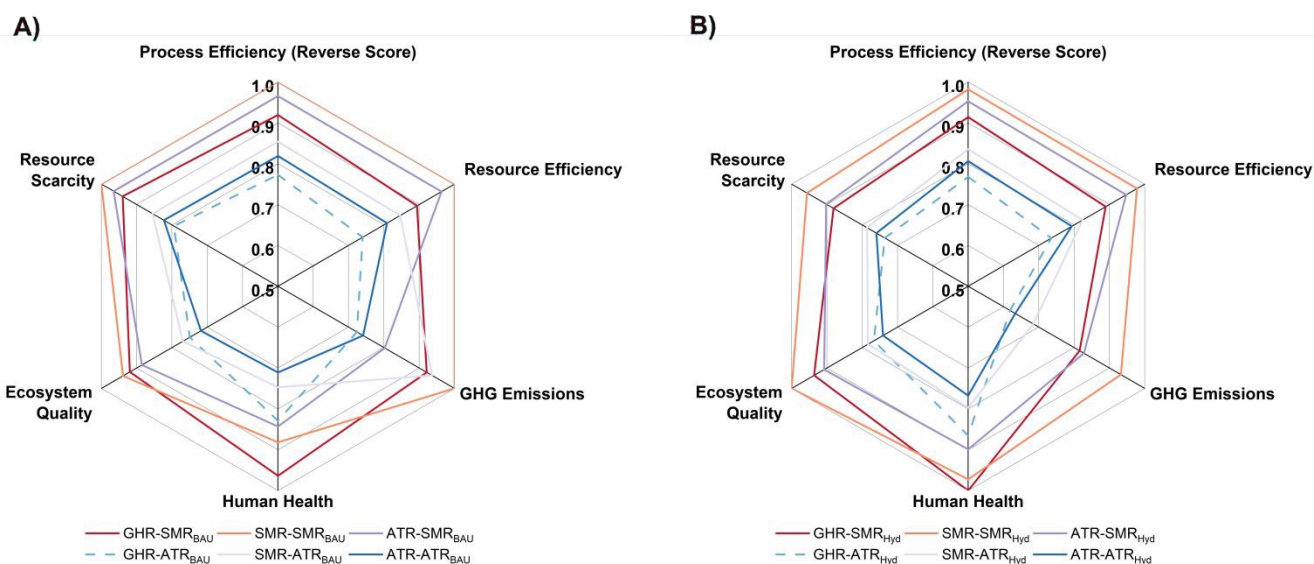
470      **Fig. 6** Sustainability Analysis of A) BAU and B) IS integrated MeOH-NH$_3$ co-production

471      flowsheets. The blue dashed line [---] in both spider plots indicates the best-performing co-

472      production flowsheet, which meets all decision criteria. This flowsheet was chosen as it has the

473      smallest internal area and, thus, provides optimum results.

474

475      Focusing on BAU operations, where there are no IS linkages among processes, the

476      SMR$_{NH3}$ cases were consistently outperformed due to higher burdens linked to all

477      indicators. Although SMR is one of the most common and widely used methods for H$_2$

478      production for MeOH and NH$_3$ production,[49] our results illustrate that ATR alternatives

479 produce more sustainable pathways, even if fossil-based natural gas is utilised. The
480 GHR-ATR$_{BAU}$ is the most compelling co-production system to utilise if using a system with
481 only fossil-based fuels.

482

483 When IS linkages with $CO_2$ and $H_2$ were introduced to BAU production, there was a
484 noticeable shift towards lower GHG emissions and resource scarcity and higher efficiency
485 indicators for all the pathways as the integration of green $H_2$ and $CO_2$ reuse reduces the
486 dependency of the fossil-based fuels without losing MeOH and $NH_3$ productivity. The
487 most attractive co-production scheme using IS and green $H_2$ was the GHR-ATR$_{Hyd}$
488 system while ATR-ATR$_{Hyd}$ flowsheets show strong competitiveness as burden-shifting is
489 reduced. Implementation of the GHR-ATR$_{Hyd}$ system can lead to high process and
490 resource efficiency and there would be a reduction in the overall GHG emissions
491 compared to traditional systems where SMR technology is used. However, if existing
492 industrial plants were retrofitted with these technologies, significant capital expenditure
493 and the development of hydrogen production plants would be required and hence these
494 are limitations to the implementation of the system. It should be noted that this system
495 has shown to be best-performing co-production system compared to other systems, but
496 these findings are valid only at the capacities considered in the study. Therefore, lower
497 scale production systems may not show the same findings. Overall, our results illustrate
498 the need for cleaner supply chains (*e.g. renewable energy*) within co-production schemes
499 with IS as pathways to sustainable, large-scale production of MeOH and $NH_3$.

500

501 To achieve higher levels of IS and sustainability, companies must be willing to work
502 together to develop these co-production systems. Although IS can be adopted using a
503 top-down approach, it is recommended that companies employ a bottom-up approach
504 where there is self-organisation of the IS exchanges amongst the plants. A recent
505 example of self-organisation of IS for the co-production of MeOH and $NH_3$ is the
506 partnership between KBR and Johnson Matthey.[40] This exemplifies that companies can
507 successfully collaborate to achieve lower emissions and higher sustainability levels for
508 their companies. As with all IS relationships, there are challenges involved which include
509 technology readiness and maturity, economic factors and policy development.[50]

21

510    However, if the companies have common goals of increasing sustainability levels and

511    have the financial resources, these relationships can be nurtured and can flourish.

512    Further work can therefore be undertaken utilising supply chain optimisation of the co-

513    production schemes with techno-economic analyses to highlight the viability of IS

514    integration and hybridisation within conventional large-scale chemical production.

515

516    **Table 2** Life Cycle Inventories for BAU and IS integrated (*Hyd*) MeOH-$NH_3$ co-production cases.

517                     Functional unit (FU) = 1 kg $NH_3$.

| Technology | GHR-SMR | SMR-SMR | ATR-SMR | GHR-ATR | SMR-ATR | ATR-ATR | GHR-SMR | SMR-SMR | ATR-SMR | GHR-ATR | SMR-ATR | ATR-ATR |
|---|---|---|---|---|---|---|---|---|---|---|---|---|
| | BAU | BAU | BAU | BAU | BAU | BAU | Hyd | Hyd | Hyd | Hyd | Hyd | Hyd |
| **INPUTS- Materials** | | | | | | | | | | | | |
| **Natural Gas[a] [kg]** | 2.37 | 2.65 | 2.55 | 1.96 | 2.24 | 2.14 | 2.14 | 2.37 | 2.29 | 1.73 | 1.97 | 1.88 |
| **Water [kg]** | 1.11 | 1.81 | 0.88 | 1.61 | 2.31 | 1.38 | 1.07 | 1.66 | 0.88 | 1.57 | 2.16 | 1.38 |
| **Captured $CO_2$[b] [kg]** | - | - | - | - | - | - | | 1.41 | | | | |
| **Green $H_2$ [kg]** | - | - | - | - | - | - | 0.089 | 0.089 | 0.089 | 0.089 | 0.089 | 0.089 |
| **INPUTS- Energy** | | | | | | | | | | | | |
| **Electricity[c] [kWh]** | 1.10 | 0.20 | 0.27 | 1.35 | 0.45 | 0.52 | 1.07 | 0.31 | 0.37 | 1.31 | 0.56 | 0.62 |
| **Heating[d] [kWh]** | 4.69 | 11.22 | 5.37 | - | 6.53 | 0.68 | 4.69 | 10.15 | 5.26 | - | 5.46 | 0.57 |
| **Cooling [kWh]** | 6.49 | 9.09 | 8.09 | 5.66 | 8.26 | 7.26 | 6.37 | 8.55 | 7.70 | 5.54 | 7.71 | 6.87 |
| **OUTPUTS- MATERIALS** | | | | | | | | | | | | |
| **MeOH [kg]** | 2.71 | 2.71 | 2.71 | 2.71 | 2.71 | 2.71 | 2.71 | 2.71 | 2.71 | 2.71 | 2.71 | 2.71 |
| **$NH_3$ [kg]** | 1.00 | 1.00 | 1.00 | 1.00 | 1.00 | 1.00 | 1.00 | 1.00 | 1.00 | 1.00 | 1.00 | 1.00 |
| **Process $CO_2$ [kg]** | 1.23 | 0.34 | 1.23 | 1.47 | 0.58 | 1.47 | 0.56 | - | 0.56 | 0.80 | 0.06 | 0.80 |
| **Other $CO_2$ [kg]** | 1.22 | 2.88 | 1.71 | 0.19 | 1.85 | 0.68 | 1.26 | 2.64 | 1.67 | 0.23 | 1.61 | 0.64 |
| **CO-PRODUCT ALLOCATION[e]** | | | | | | | | | | | | |
| **MeOH** | 0.716 | 0.716 | 0.716 | 0.716 | 0.716 | 0.716 | 0.716 | 0.716 | 0.716 | 0.716 | 0.716 | 0.716 |

| | | | | | | | | | | | | |
|---|---|---|---|---|---|---|---|---|---|---|---|---|
| NH$_3$ | 0.284 | 0.284 | 0.284 | 0.284 | 0.284 | 0.284 | 0.284 | 0.284 | 0.284 | 0.284 | 0.284 | 0.284 |
| **KPIs$^f$** | | | | | | | | | | | | |
| Energy Efficiency [%] | 66.93 | 61.51 | 63.72 | 79.59 | 72.05 | 75.12 | 67.31 | 62.68 | 64.58 | 80.14 | 73.65 | 76.32 |
| Resource Efficiency [MJ/kg$_{products}$] | 31.28 | 35.00 | 33.71 | 25.89 | 29.61 | 28.31 | 31.13 | 34.24 | 33.16 | 25.74 | 28.85 | 27.76 |

518 $^a$Total Natural gas required both as feedstock and utility heating purposes; $^b$Captured CO$_2$ from Natural Gas Power
519 Plant; $^c$Net Electricity consumed considering total power generated within flowsheets; $^d$Net Heating consumed
520 considering total heat produced from purge gas, NH$_3$ boil-off and total heat required by natural gas; $^e$Economic
521 allocation considering MeOH price = USD 0.679/kg,[51] NH$_3$ price = USD 0.73/kg;[52] Energy and Resource efficiencies
522 evaluated at LHV$_{natgas}$ = 49 MJ/kg;[53] LHV$_{MeOH}$ = 22.7 MJ/kg;[54] LHV$_{NH3}$ = 18.8 MJ/kg;[55] LHV$_{H2}$ = 120.2 MJ/kg.[53]

523

## 4. Conclusion

525 The inherent flexibility of IS-integrated co-production systems, which allow for seamless
526 incorporation of renewable energy sources, positions them as pivotal players in the
527 transition toward sustainable industrial practices. Our study underscores the
528 transformative potential of IS in reshaping production within the existing MeOH and NH$_3$
529 industries. By integrating green H$_2$ produced through electrolysis and utilising CO$_2$ from
530 NH$_3$ synthesis, we have demonstrated a viable pathway for significantly reducing the
531 carbon footprint of these essential chemical industries. A detailed analysis revealed that
532 the application of IS, mainly through the ATR$_{NH3}$ configurations, has shown superior
533 performance in energy efficiency and reduced resource intensity compared to
534 conventional SMR$_{NH3}$ systems. In contrast, IS-integrated flowsheets for MeOH
535 demonstrate significant reductions in natural gas use and heating requirements albeit with
536 an 8% increase in electricity consumption due to E-methanol production. These changes
537 result in an average 28% reduction in total CO$_2$ emissions across IS cases compared to
538 BAU operations. Notably, the trade-offs between electrification and heating offer
539 substantial benefits for low-carbon NH$_3$ production, with the GHR-ATR$_{Hyd}$ configuration
540 achieving a noteworthy reduction in natural gas consumption and CO$_2$ emissions,
541 highlighting its potential as a leading approach for low-carbon chemical manufacturing.

542 General trends indicate that EE increases and RI decreases in the order of GHR > ATR

543 > SMR, with $ATR_{NH3}$ outperforming $SMR_{NH3}$ in most metrics. Specifically, the GHR-

544 $ATR_{BAU}$ configuration emerges as the most energetically favourable. While IS promotes

545 efficient energy use, it is crucial to recognise that the GHR-$ATR_{BAU}$ systems excel beyond

546 other configurations, except for its hybrid variant GHR-$ATR_{Hyd}$. This underscores the

547 necessity for comprehensive energy analysis and trade-off assessments in co-production

548 schemes. In BAU co-production setups, the primary hotspots are linked to natural gas

549 consumption and direct $CO_2$ emissions, with similar trends observed in hybrid systems,

550 albeit with slightly lower impacts. GHG impacts improve in the sequence GHR-$ATR_{Hyd}$ >

551 $ATR-ATR_{Hyd}$ > $SMR-ATR_{Hyd}$ > $GHR-SMR_{BAU}$ > $ATR-SMR_{BAU}$ > $SMR-SMR_{BAU}$, aligning

552 with energy and resource efficiency results. Although the benefits of IS are primarily

553 realised through green $H_2$ integration, the inherent flexibility of IS-integrated co-production

554 flowsheets supports greater E-methanol integration as renewable electricity scales up,

555 enabling more sustainable MeOH and $NH_3$ production.

556 Looking ahead, future work offers significant opportunities to optimize IS-integrated

557 systems and advance their sustainability. Building on the demonstrated environmental

558 benefits of the IS pathway, key areas of focus include integrating GHR ammonia systems

559 to explore additional low-carbon co-production schemes and conducting techno-

560 economic analyses to assess their scalability and financial feasibility. Supply chain

561 optimization processes can also be employed to determine the optimal mix of

562 technologies and address logistical challenges, while incorporating life cycle costing will

563 provide a comprehensive assessment of long-term economic and environmental impacts.

564 Furthermore, identifying and addressing potential technical bottlenecks, such as process

565 inefficiencies or material compatibility issues, will be critical. These efforts, combined with

566 strategies to scale and commercialize IS systems, will help bridge the gap between

567 research and industrial application, ultimately supporting broader absolute sustainability

568 goals.

569 Overall, ATR configurations demonstrate superior performance across human health and

570 ecosystem quality, whereas GHR and SMR technologies show less favourable outcomes.

571 Despite potential burden shifting, the overall impact remains positive, with the GHR-

24

572   $ATR_{Hyd}$ approach emerging as the most favourable production method compared to
573   current BAU processes - advancing decarbonisation efforts within the MeOH and $NH_3$
574   industries. Ultimately, this study demonstrates that IS is a viable strategy for the cleaner
575   co-production of MeOH and $NH_3$, offering a transferable model for sustainable chemical
576   production in other carbon-intensive industries, advocating for a promising pathway
577   toward achieving net-zero emissions and defossilising chemical sectors.

578 **Appendix A. Supplementary data**

579 All specific data supporting this article have been included as part of the Supplementary

580 Information.

581 **Conflicts of interest**

582 There are no conflicts to declare.

583 **Acknowledgements**

587

588

589 **References**

590 1.    J. Mahabir, N. Samaroo, M. Janardhanan and K. Ward, *Journal of CO2 Utilization*,
591       2022, **66**, 102302.
592 2.    UNCC,    What    is    the    Paris    Agreement?,    https://unfccc.int/process-and-
593       meetings/the-paris-agreement, (accessed 19/07/2024).
594 3.    W. Lamb, F, T. Wiedmann, J. Pongratz, R. Andrew, M. Crippa, J. Oliver, G, J, D.
595       Widenhofer, G. Mattiol, A. Khourdajie, A and J. House, *Environ. Res. Lett.*, 2021,
596       **16**, 073005.
597 4.    R. Cao, K. Lueck, C. Musso and V. Sarathy, The chemicals industry of tomorrow:
598       Collaborate    to    innovate,    https://www.mckinsey.com/industries/chemicals/our-
599       insights/the-chemicals-industry-of-tomorrow-collaborate-to-innovate,    (accessed
600       02/04/2024).
601 5.    F. Dalena, A. Senatore, A. Marino, A. Gordano, M. Basile and A. Basile, in
602       *Methanol*,    eds.    A.    Basile    and    F.    Dalena,    Elsevier,    2018,    DOI:
603       https://doi.org/10.1016/B978-0-444-63903-5.00001-7, pp. 3-28.
604 6.    S. A. Bhat and J. Sadhukhan, *AIChE Journal*, 2009, **55**, 408-422.
605 7.    K. Narine, J. Mahabir, N. Koylass, N. Samaroo, S. Singh-Gryzbon, A. Baboolal, M.
606       Guo and K. Ward, *Journal of CO2 Utilization*, 2021, **44**, 101399.
607 8.    T. Klein, *Methanol: A Future-Proof Fuel*, Future Fuel Strategies, 2020.
608 9.    D. R. MacFarlane, P. V. Cherepanov, J. Choi, B. H. R. Suryanto, R. Y. Hodgetts,
609       J. M. Bakker, F. M. Ferrero Vallana and A. N. Simonov, *Joule*, 2020, **4**, 1186-1205.
610 10.   Precedence Research, Ammonia Market (By Product Form: Liquid, Gas, Powder;
611       By Application: Fertilizers, Refrigerants, Pharmaceuticals, Textile, Others) - Global
612       Industry Analysis, Size, Share, Growth, Trends, Regional Outlook, and Forecast
613       2023-2032,    https://www.precedenceresearch.com/ammonia-market    (accessed
614       04/11/2023).

615  11.  H. Bouaboula, M. Ouikhalfan, I. Saadoune, J. Chaouki, A. Zaabout and Y. Belmabkhout, *Energy Rep.*, 2023, **9**, 4507-4517.

617  12.  A. O. Oni, T. Giwa, C. Font-Palma and D. A. Fadare, *Int. J. Greenhouse Gas Control*, 2023, **123**, 103819.

619  13.  S. Ghavam, M. Vahdati, I. A. G. Wilson and P. Styring, *Frontiers in Energy Research*, 2021, **9**.

621  14.  IRENA and MI, *Innovation Outlook: Renewable Methanol*, International Renewable Energy Authority, Abu Dhabi, 2021.

623  15.  Y. Khojasteh-Salkuyeh, O. Ashrafi, E. Mostafavi and P. Navarri, *Journal of CO2 Utilization*, 2021, **50**, 101608.

625  16.  R. A. Frosch and N. E. Gallopoulos, *Scientific American*, 1989, **261**, 144-153.

626  17.  A. Wolf and M. Wallén, *Progress in Industrial Ecology, An International Journal*, 2008, **5**.

628  18.  M. Martin, *Journal of Industrial Ecology*, 2019, **24**, 626 - 638.

629  19.  A. Neves, R. Godina, S. G. Azevedo and J. C. O. Matias, 2020.

630  20.  T. G. Lee Chan and D. A. Janes, *Carbon Capture Sci. Technol.*, 2023, **7**, 100109.

631  21.  S. C. D'Angelo, S. Cobo, V. Tulus, A. Nabera, A. J. Martín, J. Pérez-Ramírez and G. Guillén-Gosálbez, *ACS Sustainable Chemistry & Engineering*, 2021, **9**, 9740-9749.

634  22.  A. Crivellari, V. Casson Moreno, V. Cozzani and I. Dincer, *Journal of Cleaner Production*, 2021, **293**, 126226.

636  23.  A. Valera-Medina, F. Amer-Hatem, A. K. Azad, I. C. Dedoussi, M. de Joannon, R. X. Fernandes, P. Glarborg, H. Hashemi, X. He, S. Mashruk, J. McGowan, C. Mounaim-Rouselle, A. Ortiz-Prado, A. Ortiz-Valera, I. Rossetti, B. Shu, M. Yehia, H. Xiao and M. Costa, *Energy & Fuels*, 2021, **35**, 6964-7029.

640  24.  S. E. Hosseini and M. A. Wahid, *International Journal of Energy Research*, 2020, **44**, 4110-4131.

642  25.  T. I. Sigfusson, *Philosophical Transactions of the Royal Society A: Mathematical, Physical and Engineering Sciences*, 2007, **365**, 1025-1042.

644  26.  S. Satyapal, N. Ruustagi, T. Green, M. Melaina, M. Penev and M. Koleva, *Journal*, 2023.

646  27.  EIA, Production of Hydrogen, https://www.eia.gov/energyexplained/hydrogen/production-of-hydrogen.php, (accessed 25/07/2024).

649  28.  N. Armaroli and V. Balzani, *ChemSusChem*, 2011, **4**, 21-36.

650  29.  W. Flood, *Energy & Environment*, 2012, **23**, 1097-1104.

651  30.  R. Kleijn and E. van der Voet, *Renewable and Sustainable Energy Reviews*, 2010, **14**, 2784-2795.

653  31.  J. Flaig, 5 major challenges in the hydrogen economy in 2024 – and 5 potential solutions, https://www.imeche.org/news/news-article/5-major-challenges-in-the-hydrogen-economy-in-2024-and-5-potential-solutions#:~:text=Of%20the%20major%20challenges%20in,to%209.8TWh%20by%202035., (accessed 26/07/2024).

658  32.  Office of Energy Efficiency & Renewable Energy, Chemical and Petrochemical Manufacturing, https://www.energy.gov/eere/iedo/chemical-and-petrochemical-manufacturing).

RSC Sustainability Accepted Manuscript

661  33.  Louisiana Economic Development, Process Industries, https://www.opportunitylouisiana.gov/key-industry/process-industries, (accessed 17/07/2024).

664  34.  A. D. Blodgett, *Local Environment*, 2006, **11**, 647-661.

665  35.  B. F. Snyder, M. Layne and D. E. Dismukes, *International Journal of Greenhouse Gas Control*, 2020, **93**, 102885.

667  36.  U.S. Energy Information Administration, *Journal*, 2023.

668  37.  Louisiana Economic Development, Louisiana Solar Power Generation is Growing, https://www.opportunitylouisiana.gov/key-industry/energy/energy-diversity/solar, (accessed 18/07/2024).

671  38.  N. Samaroo, N. Koylass, M. Guo and K. Ward, *Green Chemistry*, 2020, **22**, 6547-6559.

673  39.  A. Liquide, Air Liquide and KBR to offer ATR-based low-carbon ammonia and hydrogen technologies, https://www.airliquide.com/group/press-releases-news/2023-07-19/air-liquide-and-kbr-offer-atr-based-low-carbon-ammonia-and-hydrogen-technologies, (accessed November 7, 2024).

677  40.  J. Matthey, Methanol and ammonia co-production, https://matthey.com/products-and-markets/chemicals/methanol/methanol-and-ammonia-co-production, (accessed November 4, 2023).

680  41.  A. González-Garay, M. S. Frei, A. Al-Qahtani, C. Mondelli, G. Guillén-Gosálbez and J. Pérez-Ramírez, *Energy & Environmental Science*, 2019, **12**, 3425-3436.

682  42.  M. Institute, Renewable Methanol, https://www.methanol.org/renewable/, (accessed July 2, 2024).

684  43.  Topsoe, SynCOR Ammonia™ - New process for grassroots plants, https://www.topsoe.com/our-resources/knowledge/our-products/process-licensing/syncor-ammoniatm-new-process-for-grassroots-plants, (accessed July 3, 2024).

688  44.  P. J. Dahl, SynCOR Hydrogen™ The Optimal Solution for Blue, https://globalsyngas.org/wp-content/conference-presentations/2020/2020-w1-d2-m1-JD-SynCOR.pdf, (accessed June 5, 2024).

691  45.  Z. Haonan, Z. Cunquan, Z. Meng and S. Peng-cheng, *Cryogenics*, 2020, **106**, 103022.

693  46.  K. Bhagaloo, R. Ali, A. Baboolal and K. Ward, *Sustain. Energy Technol. Assessments*, 2022, **51**, 101910.

695  47.  M. Temkin and V. Pyzhev, *J. Phys. Chem.*, 1939, **13**, 851-857.

696  48.  M. A. J. Huijbregts, Z. J. N. Steinmann, P. M. F. Elshout, G. Stam, F. Verones, M. Vieira, M. Zijp, A. Hollander and R. van Zelm, *Int. J. Life Cycle Assess.*, 2017, **22**, 138-147.

699  49.  P. Nikolaidis and A. Poullikkas, *Renewable and Sustainable Energy Reviews*, 2017, **67**, 597-611.

701  50.  M. Demartini, F. Tonelli and K. Govindan, *Cleaner Logistics and Supply Chain*, 2022, **3**, 100020.

703  51.  Methanex, Pricing, https://www.methanex.com/about-methanol/pricing/, (accessed July 12, 2024).

705   52.   B.              Analytiq,         Ammonia         Price         Index,
706         https://businessanalytiq.com/procurementanalytics/index/ammonia-price-index/,
707         (accessed July 5, 2024).
708   53.   W.   N.   Association,   Heat   Values   of   Various   Fuels,   https://world-
709         nuclear.org/information-library/facts-and-figures/heat-values-of-various-fuels,
710         (accessed July 4, 2024).
711   54.   L. Eggemann, N. Escobar, R. Peters, P. Burauel and D. Stolten, *J. Clean. Prod.*,
712         2020, **271**, 122476.
713   55.   C. Zamfirescu and I. Dincer, *J. Power Sources*, 2008, **185**, 459-465.
714

RSC Sustainability Accepted Manuscript

# Towards Flexible Large-Scale Environmentally Sustainable Methanol and Ammonia Production using Industrial Symbiosis

Joshua Magson[a], Thérèse Lee Chan[b], Akeem Mohammed[b],  Keeran Ward*[a]

[a]School of Chemical and Process Engineering (SCAPE), University of Leeds, Leeds, LS2 9JT, U.K

[b]Department of Chemical Engineering, University of the West Indies, St. Augustine, Trinidad, WI.

*Corresponding author; Email: k.r.ward@leeds.ac.uk;

## Data Availability Statement

All specific data supporting this article have been included as part of the Supplementary Information.